

## THE MAGNETIC FIELD IN THE CLASS 0 PROTOSTELLAR DISK OF L1527

DOMINIQUE M. SEGURA-COX<sup>1</sup>, LESLIE W. LOONEY<sup>1</sup>, IAN W. STEPHENS<sup>1,2</sup>, MANUEL FERNÁNDEZ-LÓPEZ<sup>1,3</sup>, WOJIN KWON<sup>4</sup>, JOHN J. TOBIN<sup>5</sup>, ZHI-YUN LI<sup>6</sup>, RICHARD CRUTCHER<sup>1</sup>

*Accepted by ApJL*

### ABSTRACT

We present subarcsecond ( $\sim 0.35''$ ) resolved observations of the 1.3 mm dust polarization from the edge-on circumstellar disk around the Class 0 protostar L1527. The inferred magnetic field is consistent with a dominantly toroidal morphology; there is no significantly detected vertical poloidal component to which observations of an edge-on disk are most sensitive. This suggests that angular momentum transport in Class 0 protostars (when large amounts of material are fed down to the disk from the envelope and accreted onto the protostar) is driven mainly by magnetorotational instability rather than magnetocentrifugal winds at 50 AU scales. In addition, with the data to date there is an early, tentative trend that  $R > 30$  AU disks have so far been found in Class 0 systems with average magnetic fields on the 1000 AU scale strongly misaligned with the rotation axis. The absence of such a disk in the aligned case could be due to efficient magnetic braking that disrupts disk formation. If this is the case, this implies that candidate Class 0 disk systems could be identified by the average magnetic field direction at  $\sim 1000$  AU spatial scales.

*Subject headings:* ISM: individual objects (L1527) — ISM: magnetic fields — polarization — stars: protostars

### 1. INTRODUCTION

Circumstellar disks are a key component of the star formation process and are fundamental for accretion and angular momentum distribution during the early phases of star formation. Class 0 objects are the youngest and most embedded protostars, and circumstellar disks form at this earliest stage of star formation if angular momentum is conserved during cloud collapse (e.g., Cassen & Moosman 1981). Class 0 disks are extremely obscured by envelopes, which contribute  $\gtrsim 90\%$  of the total emission (Looney et al. 2000), making the search for Class 0 disks challenging. However, observations of Class 0 disks and their properties are essential to provide the initial conditions for mass accretion onto the central protostar and planet formation. To date, only a few Class 0 systems have observed disks with clear Keplerian rotation (e.g., Tobin et al. 2012; Murillo et al. 2013; Codella et al. 2014); L1527, VLA 1623, and HH212 have Keplerian disks with  $R > 30$  AU, sizes larger than magnetic braking models predict.

In addition to the properties of young disks and envelopes, the morphology and strength of the magnetic field in these systems also play an important role in star formation (e.g., Crutcher 2012). For example, the morphology of the magnetic field in the young disk provides important clues into angular momentum trans-

port: disk accretion driven by magnetorotational instabilities (MRI, Balbus & Hawley 1998) favor toroidal fields while angular momentum removal via magnetocentrifugal winds arising from the disk favor poloidal fields (e.g., Blandford & Payne 1982). The magnetic field morphology in the envelope and disk can be inferred; dust grains preferentially align with their long-axis perpendicular to the magnetic field, causing the dust emission to be polarized (e.g., Lazarian 2007). An interferometric survey of dust polarization around 26 low-mass Class 0/I protostars has been recently conducted (TADPOL, Hull et al. 2013, 2014). For these sources, the average magnetic field axes are generally misaligned with the rotation axes of the systems (as proxied by the outflow). In the case of L1527 and VLA 1623, TADPOL observations show that the magnetic field lines are perpendicular to the outflows. However, the TADPOL results only probe envelope size scales and do not approach disk scales. The magnetic field morphology on smaller scales has been observed in the Class 0 protostars L1157 and IRAS 16293-2422 B. L1157, whose disk is yet to be resolved and has  $R < 20$  AU (Tobin et al. 2013a), has vertical poloidal component magnetic fields aligned with the rotation axis of the system in the inner envelope (Stephens et al. 2013). IRAS 16293-2422 B—which is thought to have a face-on disk and hence no clear Keplerian motion—has resolved observations of the candidate disk with a polarization pattern indicative of a toroidal magnetic field component (Rao et al. 2014), although the face-on geometry makes the detection of any vertical poloidal component impossible.

In this Letter, we present high-resolution CARMA 1.3 mm dust polarimetric observations of the Class 0 protostar L1527. Lower-resolution CARMA 1.3 mm polarimetric observations of L1527 were previously conducted as a part of the TADPOL survey, probing the magnetic field morphology on  $\sim 1000$  AU envelope size scales. Here we report the magnetic field morphology on  $\sim 50$  AU disk

<sup>1</sup> Department of Astronomy, University of Illinois, Urbana, IL 61801, USA; segurac2@illinois.edu

<sup>2</sup> Institute for Astrophysical Research, Boston University, Boston, MA 02215, USA

<sup>3</sup> Instituto Argentino de Radioastronomía, CCT-La Plata (CONICET), C.C.5, 1894, Villa Elisa, Argentina

<sup>4</sup> SRON Netherlands Institute for Space Research, Landleven 12, 9747 AD Groningen, The Netherlands

<sup>5</sup> National Radio Astronomy Observatory, Charlottesville, VA 22903, USA

<sup>6</sup> Astronomy Department, University of Virginia, Charlottesville, VA 22904, USA

size scales. The data presented are the first detection of polarized dust emission emanating directly from a Class 0 Keplerian disk.

## 2. OBSERVATIONS

CARMA 1 mm full-Stokes observations of L1527 were obtained in 6 tracks of the B array ( $\sim 0.35''$  resolution) from 2013 December 9–13 and 15 for a total of 21 hours on-source. The correlator was set up with a local oscillator frequency of 233.731 GHz and four 500 MHz-wide bands centered at intermediate frequency values of 2.187, 2.740, 4.716, and 5.544 GHz. We used the MIRIAD software package (Sault et al. 1995) to reduce the data. The polarization calibration followed the standard process for CARMA (Hull et al. 2014). The phase and polarization leakage calibrator for all tracks was 0510+180. The preferred bandpass calibrator was 3C84, and 3C454.3 was used when 3C84 was unavailable. For most tracks, the flux calibrator was MWC349 with a calibration accuracy estimation of  $\sim 15\%$ , but only statistical uncertainties are considered in this Letter. When this calibrator was not observed, the flux was interpolated from the observations of MWC349 in other tracks. To maximize sensitivity, maps of the 4 Stokes parameters (I, Q, U, and V) were created using natural weighting. From these, we derive the polarization position-angle and intensity maps. We also generated new maps of L1527 data from the TADPOL survey (Hull et al. 2014). The data include 5 tracks between 2011 May and 2013 April in D and E arrays.

## 3. RESULTS

The 1.3 mm dust emission map of L1527 is presented in Figure 1 and is consistent with the known edge-on disk (Tobin et al. 2013b). The disk has been resolved previously at 3.4 mm and  $870 \mu\text{m}$  (Tobin et al. 2012) and also has been shown to have Keplerian motion and a radius of 54 AU (Ohashi et al. 2014, in press). Our observations are the first resolved detection of the disk at 1.3 mm. At a resolution of  $\sim 0.35''$  and a distance of 140 pc (Loinard et al. 2007), our interferometric observations probe L1527 on size scales of  $\sim 50$  AU. An elliptical Gaussian fit to the high-resolution 1.3 mm Stokes I data measures a deconvolved size of  $0.53'' \times 0.23''$  with position angle of  $5.2^\circ$  (PA, measured counterclockwise), consistent with the deconvolved sizes at 3.4 mm,  $870 \mu\text{m}$  (Tobin et al. 2013b), and 1.3 mm (Ohashi et al. 2014, in press). In addition, our flux density at 1.3 mm ( $139 \pm 4$  mJy) is consistent with detection of the L1527 disk seen in Tobin et al. (2013b). Using the measured fluxes at 3.4 mm and  $870 \mu\text{m}$  and the derived  $\beta=0$  from Tobin et al. (2013b), we can estimate the expected disk emission at 1.3 mm (116 mJy and 96 mJy, respectively), which is congruent with our measured 1.3 mm fluxes when taking account a 20% extrapolating and amplitude uncertainty. Based on this evidence, our observations are dominated by disk emission of the L1527 system, with little contamination from the large-scale envelope emission.

We detect dust polarization of the young disk over 2 synthesized beams with an average polarization of  $2.5\% \pm 0.6\%$  and a position angle of  $5^\circ \pm 5^\circ$  measured counterclockwise from north, aligning well with the Stokes I elliptical Gaussian fitted position angle of  $5.2^\circ \pm 0.4^\circ$ . The inferred magnetic field (with polarization vectors rotated by  $90^\circ$ ) is shown in Figure 1. The mor-

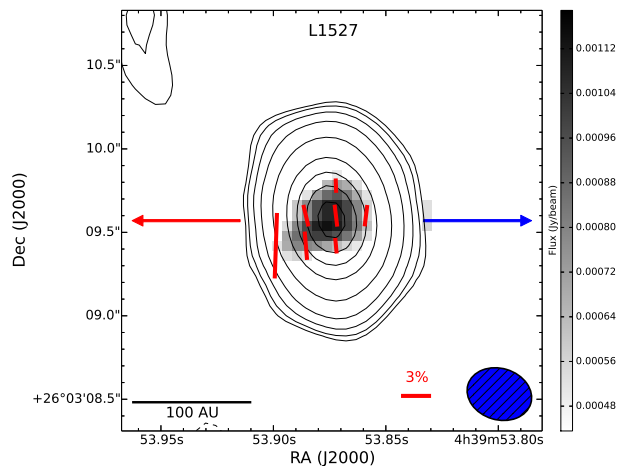


**Figure 1.** Polarimetric map (polarization vectors rotated by  $90^\circ$  to show inferred magnetic field orientation) of the L1527 disk from CARMA data with a  $0.39'' \times 0.31''$  beam. Fractional polarization vectors  $\geq 3\sigma$  displayed. Contours are Stokes I data with levels of  $[-6, -4, -3, 3, 4, 6, 10, 20, 40, 60, 80, 100] \times \sigma$ ,  $\sigma = 0.45$  mJy beam $^{-1}$ . Grayscale shows the polarized intensity  $\geq 3\sigma$ . Outflows in the plane of the sky are marked by red and blue arrows.

phology of the inferred field is parallel to the disk axis, as is expected from an edge-on toroidal field—uniform and aligned with the disk. We compare a uniform field at a  $5^\circ$  PA (the same as the dust emission) to the data and find a reduced  $\chi^2 < 1$ . The polarization fraction of the circumstellar disk of L1527 is larger than the 1.4% polarization fraction found in the face-on candidate disk of IRAS 16293-2422 B (Rao et al. 2014), although the lower polarization fraction of IRAS 16293-2422 B may be due in part to beam-averaging; due to orientation, an edge on toroidal field is less beam-averaged as the vectors are more uniform. Our polarization percentage is similar to the theoretically predicted 2-3% polarization fraction found in simulations of magnetized disks (Cho & Lazarian 2007). On the other hand, observations of the disks of older T Tauri systems have much lower polarization percentages  $< 1\%$  (Hughes et al. 2009, 2013), which may be an outcome of dust processing or de-alignment mechanisms during disk evolution (Stephens et al. 2014).

A uniform field in the plane of the disk is physically unlikely for a rapidly-rotating, Keplerian disk system. One expects either poloidal, toroidal, or a combination of the two in such a disk (e.g. Balbus & Hawley 1998; Königl & Pudritz 2000). For an edge-on disk, observations are most sensitive to vertical poloidal field components because they are expected to vertically thread the disk and thus lay roughly in the plane of the sky. However, our data does not exhibit any obvious poloidal morphology which would be perpendicular to the disk. To show that a toroidally dominant morphology is consistent with our observations, we compare to a purely toroidal, a purely vertical poloidal, and combinations of toroidal and vertically poloidal toy models (see caption of Figure 2 for details). We used the best-fit disk parameters of Tobin et al. (2013b): disk inclination angle of  $85^\circ$ ,  $0^\circ$  PA,  $M_{\text{disk}} = 0.0075 M_\odot$ ,  $R_{\text{inner}} = 0.1$  AU,  $R_{\text{outer}} = 125$  AU, and stellar and accretion luminosity of  $2.75 L_\odot$ . The temperature distribution was calculated using the Monte-Carlo radiative code RADMC-3D

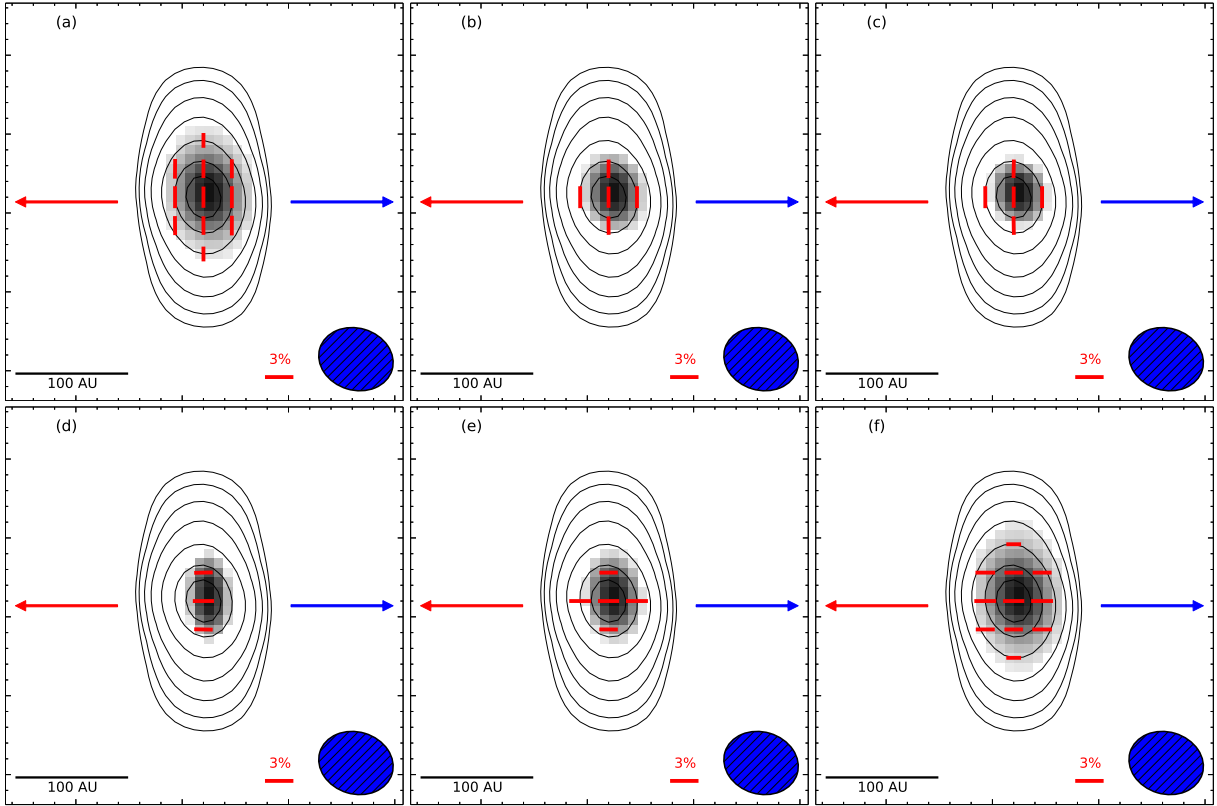


**Figure 2.** Synthetic maps of the L1527 disk magnetic field morphology. Contours, grayscale, and vectors are the same as Figure 1. (a) Toroidal field only, (b) 70% toroidal/30% vertical poloidal field, (c) 60%/40%, (d) 50%/50%, (e) 40%/60%, (f) vertical poloidal field only.

(Dullemond & Dominik 2004). The Stokes I, Q, and U maps were numerically solved using dust radiative transfer in the disk along the line of sight with an assumed constant polarization fraction. The magnetic field vectors at each integral element have been tilted and rotated based on the inclination and position angles of the disk model. Finally, all maps are convolved with the synthesized beam from the polarization observations (for more details see Stephens et al. 2014). As shown in Figure 2, the detected polarization is characterized well by our toroidally dominant toy models with up to 40% poloidal field (Figure 2a, 2b, 2c), with a reduced  $\chi^2 \sim 1.8$  for all three cases as fit to the morphology in the image plane with the vectors shown in Figure 1. The scenarios where the vertical poloidal component is equally strong as the toroidal component (Figure 2d) or the vertical poloidal component is dominant (Figure 2e, 2f) do not reproduce the observed magnetic field morphology. The purely toroidal simple model exhibits more extensive polarization than the observations, which is likely due to our assumption of constant polarization in the disk.

#### 4. DISCUSSION

In quiescent (non-turbulent) systems with aligned magnetic field and disk rotation axes, magnetic braking can have a significant effect on the infalling material in the ideal MHD limit, removing angular momentum (Mellon & Li 2008; Hennebelle & Fromang 2008), and suppressing growth of the early circumstellar disk by allowing larger accretion rates (Li et al. 2011). Magnetic braking can be so effective in Class 0 sources that rotationally supported disks are limited to  $R < 10$  AU (e.g.,

Dapp & Basu 2010), only reaching  $R \sim 100$  AU at the end of the main mass accretion phase when the envelope is less massive and magnetic braking becomes inefficient (e.g., Dapp et al. 2012; Mellon & Li 2009; Machida et al. 2011). Conversely to this prediction, Keplerian disks have been detected in Class 0 sources with sizes larger than expected from magnetic braking models. L1527 and VLA 1623 have disk sizes of  $R \sim 54$  AU and  $R \sim 189$  AU respectively (Ohashi et al. 2014, in press; Murillo et al. 2013), and HH212 has a disk of  $R > 30$  AU (Codella et al. 2014).

There are large disks in some young systems, suggesting that significant magnetic braking has not happened, has already occurred, or the magnetic field has diffused to the point where a  $R > 10$  AU disk could form. On the other hand, similar high resolution observations of the Class 0 protostar L1157 have not detected a circumstellar disk down to spatial resolutions of  $\sim 15$  AU (Tobin et al. 2013a). This result suggests that magnetic braking may have been more significant in L1157 than L1527. Of course, there are differences in age since L1527 is an older source and could have been classified as a Class I source, were it not viewed edge-on (Tobin et al. 2008). What is clear is that some Class 0 sources have  $R > 10$  AU circumstellar disks and others do not. Such differences in disk size could be a consequence of misalignment between the magnetic field and rotation axis, which modifies the strength of magnetic braking (Hennebelle & Ciardi 2009; Joos et al. 2012; Li et al. 2013; Krumholz et al. 2013).

To better understand the role of the magnetic field in the early disk and envelope, we can compare the magnetic field of L1527 presented here with the larger-scale

**Table 1**  
B array and TADPOL Results

Data Set	Stokes I Flux (mJy)	Polarized Flux (mJy)	$P_{\%}$ (%)	PA ( $^{\circ}$ )	Beam ( $''$ )
B array	139 $\pm$ 4	1.1 $\pm$ 0.2	2.5 $\pm$ 0.6	5 $\pm$ 5	0.39 $\times$ 0.31
TADPOL	188 $\pm$ 5	2.3 $\pm$ 0.3	2.8 $\pm$ 0.7	1 $\pm$ 5	2.63 $\times$ 2.26

**Note.** — Uncertainties are statistical. Results were found using data  $>3\sigma$ . Position angles are measured counterclockwise. Stokes I flux is measured across the entire disk or inner envelope; polarized flux and  $P_{\%}$  are measured in the polarized region only.

magnetic field detected with TADPOL (Figure 3 and Table 1). When comparing the polarization at 1000 AU and 50 AU, the two scales have the same average field angle: perpendicular to the outflow and well aligned with the disk plane. The higher resolution observations have less than half of the polarized emission, which suggests we are resolving out large-scale emission. The projected field morphology on the 1000 AU scale is consistent with the view that the initial magnetic field on this scale is greatly misaligned with respect to the rotation axis, although it is also possible that the field on this scale is already modified by the collapsing and rotating motions in the envelope. The magnetic fields on even larger scales are expected to be affected less by rotation and collapse, and are more likely to keep their initial configuration. The fields are better traced by single dish observations using SHARP on CSO Davidson et al. (2011) and SCUPOL on JCMT (Figure 17 of Hull et al. 2014; Matthews et al. 2009). These single dish data are modeled by Davidson et al. (2014, in press) together with CARMA data; we refer the reader to that paper for a detailed discussion of the magnetic field on large-scales. In any case, on the small scale of the disk, the available data are consistent with the field being predominantly toroidal, and such a toroidally dominant disk magnetic field is also consistent with the magnetorotational instability (e.g., Balbus & Hawley 1998) driving accretion during the main accretion phase. We do not detect significant vertical poloidal component fields that are needed to launch magnetocentrifugal winds; such winds are probably not the dominant driver of angular momentum transport during the main accretion phase at the  $\sim 50$  AU size scale. On the other hand, a disk wind would likely be launched from the disk upper layers that are not well traced by our observations, which are most sensitive to the dust in the midplane. If the poloidal field is somehow limited to the surface layers, then our observations would be less constraining on the existence or absence of a disk wind.

With dust polarization observations and high-resolution searches for disks, we can compare the magnetic field orientations and morphologies with disk properties. L1527, VLA 1623, and L1157 have all been observed with CARMA dust polarization at 500 AU or better resolution (Hull et al. 2014). L1527 and VLA 1623, the first two Class 0 systems with known Keplerian disks, have average magnetic fields perpendicular to the rotation axes (inferred from the outflow direction). In contrast, L1157, a system with a disk  $R < 20$  AU in size, has an inferred average magnetic field parallel to the rotation axis. Although we have few examples so far (Table 2), this observational, tentative trend is intriguing and suggested from theory (e.g., Joos et al. 2012); the magnetic field morphology at the earliest stages of collapse

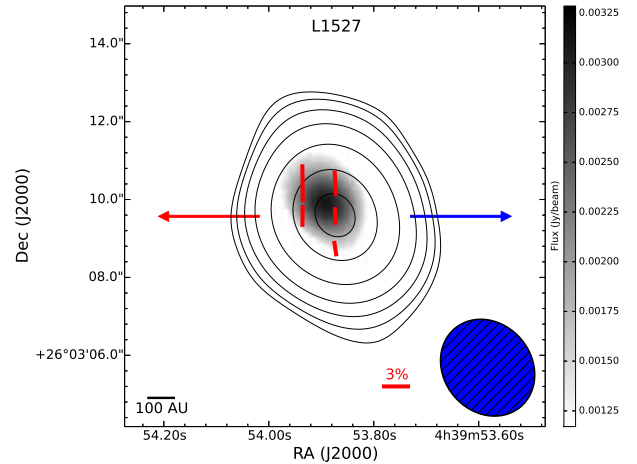


**Figure 3.** Polarimetric map of the L1527 inner envelope from the CARMA TADPOL data with a  $2.63'' \times 2.26''$  beam. Contours are Stokes I data with levels of  $[-6, -4, -3, 3, 4, 6, 10, 20, 40, 60, 80, 100] \times \sigma$ ,  $\sigma = 2.34$  mJy beam $^{-1}$ . Grayscale and vectors are the same as Figure 1.

may play an important role in the formation of the earliest disk, with strongly misaligned magnetic fields and rotation axes producing  $R > 10$  AU disks at early times. Clearly more objects are necessary to better establish this relationship.

We therefore suggest that the morphology of the magnetic field in the inner envelope ( $\sim 1000$  AU, TADPOL scales) could be another method to help identify candidate Class 0 disk sources with  $R > 10$  AU. Sources with  $R > 10$  AU disks may have a projected magnetic field on the 1000 AU scale perpendicular to the rotation axis, and the magnetic field would appear uniform for edge-on disk cases like L1527. At more oblique viewing angles at high resolution, a purely toroidal field would be observed as two maxima of fractional polarization along the axis of rotation on either side of the protostar, with the magnetic field oriented perpendicular to the outflow axis within the maxima regions (e.g., see Figure 1 in Hughes et al. 2013). A purely toroidal disk field observed directly down the rotation axis will appear as a pattern of concentric circles (e.g., Padovani et al. 2012). Sources with  $R < 10$  AU disks may have dominant vertical poloidal component fields misaligned with the axis of rotation, as is the case with L1157 with a characteristic hourglass pinch near the protostar. Such a poloidal morphology observed at viewing roughly perpendicular to the rotation axis of the system can appear either symmetric or asymmetric on either side of the pinch (Kataoka et al. 2012), especially for more oblique viewing angles: L1157 has a slight asymmetry. When a purely poloidal field is observed directly down the rotation axis, the poloidal pinch is not observed, but rather has a convergent, spoke-like mor-

**Table 2**  
Class 0 Magnetic Field Morphologies and Candidate Disks

Source	$\alpha$ (J2000)	$\delta$ (J2000)	Mag-Rot-Axis <sup>a</sup>	Candidate Disk? <sup>b</sup>	Known Keplerian?	References
L1527	04:39:53.9	26:03:09.6	Perpendicular	Yes	Yes	1,2
IRAS 16293-2422 B	16:23:22.9	-24:28:35.7	Perpendicular	Yes	No	3,4
VLA 1623	16:26:26.4	-24:24:30.5	Perpendicular	Yes	Yes	5,2
L1157	20:39:06.2	68:02:15.8	Parallel	No	No	6,2

**Note.** — <sup>a</sup> Orientation of the magnetic field compared to the rotation axis (estimated from the outflow for L1157). <sup>b</sup> Does the source have a candidate disk of  $R > 30$  AU?

**References.** — (1) Tobin et al. (2012); (2) Hull et al. (2014); (3) Zapata et al. (2013); (4) Rao et al. (2014); (5) Murillo & Lai (2013); (6) Tobin et al. (2013a)

phology. In the extreme cases of purely toroidal and purely poloidal magnetic field components, the observed morphology alone can be used to distinguish between the two cases and point towards  $R > 10$  AU candidate Class 0 disks.

## 5. CONCLUSIONS

L1527 is the first Class 0 protostar with a known Keplerian disk and direct detection of linearly polarized dust emission from the circumstellar disk, indicating magnetic fields are aligned perpendicular to the rotation axis of the disk. The magnetic field is consistent with toroidally dominant field lines. It may be that L1527's large disk arises from the strongly misaligned rotation axis and magnetic field on large scales, while aligned rotation axes and magnetic fields inhibit disk formation on  $R > 10$  AU scales. The toroidally dominant field morphology favors the magnetorotational instability (Balbus & Hawley 1998) as the dominant angular momentum transport process in Class 0 circumstellar disks.

L1527 is one of two Class 0 sources (with VLA 1623) where both magnetic fields and Keplerian disks have been detected. Both of these sources have perpendicular magnetic fields and rotation axes (Murillo & Lai 2013; Tobin et al. 2012; Hull et al. 2013) on 1000 AU scales. The alternative case is where the magnetic field and rotation axes are parallel on envelope scales, such as the Class 0 source L1157 with no disk detected down to 20 AU (Tobin et al. 2013a). It is possible that aligned magnetic fields may have braked rotation so efficiently as to inhibit the disk formation and growth at early times. The tentative trend of misaligned magnetic field and rotation axes in Class 0 systems with disks is suggestive and expected from theory, requiring follow-up to make hard conclusions about Class 0 disk formation.

We thank Chat Hull and Dick Plambeck for assistance with data reduction. This research made use of APLpy, an open-source plotting package for Python hosted at <http://aplpy.github.com>.

Support for CARMA construction was derived from the states of California, Illinois, and Maryland, the James S. McDonnell Foundation, the Gordon and Betty Moore Foundation, the Kenneth T. and Eileen L. Norris Foundation, the University of Chicago, the Associates of the California Institute of Technology, and the NSF. Ongoing CARMA development and operations are supported by the NSF under a cooperative agreement and by the CARMA partner universities.

J. Tobin acknowledges support provided by NASA

through Hubble Fellowship grant #HST-HF-51300.01-A awarded by the STScI, which is operated by AURA, Inc., for NASA, under contract NAS 5-26555. The NRAO is a facility of the NSF operated under cooperative agreement by Associated Universities, Inc.

Z.-Y. Li is supported in part by NASA 14AB38G and NSF 1313083.

## REFERENCES

- Balbus, S. A., & Hawley, J. F. 1998, *Rev. Mod. Phys.*, 70, 1
- Blandford, R. D. & Payne, D. G. 1982, *MNRAS*, 199, 883
- Cassen, P., & Moosman, A. 1981, *Icar*, 48, 353
- Cho, J., & Lazarian, A. 2007, *ApJ*, 669, 1085
- Codella, C., Cabrit, S., Gueth, F., et al. 2014, *A&A*, 568, 5
- Crutcher, R. M. 2012, *ARA&A*, 50, 29
- Dapp, W. B., & Basu, S. 2010, *A&A*, 521, L56
- Dapp, W. B., Basu, S., & Kunz, M. W., 2012, *A&A*, 541, A35
- Davidson, J.A., Li, Z.-Y., Kwon, W., et al. 2014, *ApJ*, in press
- Davidson, J.A., Novak, G., Matthews, T. G., et al. 2011, *ApJ*, 732, 97
- Dullemond, C. P., & Dominik, C. 2004, *A&A*, 417, 159
- Hennebelle, P., & Ciardi, A. 2009, *A&A*, 506, 29
- Hennebelle, P., & Fromang, S. 2008, *A&A*, 477, 9
- Hughes, A. M., Andrews, S. M., Espaillat, C., et al. 2009, *ApJ*, 698, 131
- Hughes, A. M., Hull, C. L. H., Wilner, D. J., et al. 2013, *AJ*, 145, 115
- Hull, C. L. H., Plambeck, R. L., Bolatto, A. D., et al. 2013, *ApJ*, 768, 159
- Hull, C. L. H., Plambeck, R. L., Kwon, W., et al. 2014, *ApJS*, 213, 13
- Joos, M., Hennebelle, P., & Ciardi, A. 2012, *A&A*, 543, A128
- Kataoka, A., Machida, M. N., & Tomisaka, K. 2012, *ApJ*, 761, 40
- Königl, A., & Pudritz, R. E. 2000, in *Protostars and Planets IV*, ed. V. Mannings, A. P. Boss, & S. S. Russell (Tucson, AZ: Univ. Arizona Press), 759
- Krumholz, M. R., Crutcher, R. M., & Hull, C. L. H. 2013, *ApJ*, 767, L11
- Lazarian, A. 2007, *JQSRT*, 106, 225
- Li, Z.-Y., Krasnopolsky, R., & Shang, H. 2011, *ApJ*, 738, 180
- Li, Z.-Y., Krasnopolsky, R., & Shang, H. 2013, *ApJ*, 774, 82
- Loinard, L., Chandler, C. J., Rodríguez, L. F., et al. 2007, *ApJ*, 670, 1353
- Looney, L. W., Mundy, L. G., & Welch, W. J. 2000, *ApJ*, 529, 477
- Machida, M. N., Inutsuka, S.-I., & Matsumoto, T. 2007, *ApJ*, 670, 1198
- Machida, M. N., Inutsuka, S.-I., & Matsumoto, T. 2011, *PASJ*, 63, 555
- Matthews, B. C., McPhee, C. A., Fissel, L. M., & Curran, R. L. 2009, *ApJS*, 182, 143
- Mellon, R. R., & Li, Z.-Y. 2008, *ApJ*, 681, 1356
- Mellon, R. R., & Li, Z.-Y. 2009, *ApJ*, 698, 922
- Murillo, N. M., & Lai, S.-P. 2013, *ApJL*, 764, L15
- Murillo, N. M., Lai, S.-P., Bruderer, S., et al. 2013, *A&A*, 560, 103
- Ohashi, N., Saigo, K., Aso, Y., et al., 2014, *ApJ*, in press
- Padovani, M., Brinch, C., Girart, J. M., et al. 2012, *A&A*, 543, A16
- Rao, R., Girart, J. M., Lai, S.-P., et al. 2014, *ApJL*, 780, L6

- Sault, R. J., Teuben, P. J., & Wright, M. C. H. 1995, in ASP Conf. Ser. 77, *Astronomical Data Analysis Software and Systems IV* (San Francisco, CA: ASP), 433
- Stephens, I. W., Looney, L. W., Kwon, W., et al. 2013, *ApJ*, 769, L15
- Stephens, I. W., Looney, L. W., Kwon, W., et al. 2014, *Nature*, 514, 597
- Tobin, J. J., Chandler, J. C., Wilner, D. J., et al. 2013a, *ApJ*, 779, 93
- Tobin, J. J., Hartmann, L., Calvet, N., & D'Alessio, P. 2008, *ApJ*, 679, 1364
- Tobin, J. J., Hartmann, L., Chiang, H.-F., et al. 2012, *Nature*, 492, 83
- Tobin, J. J., Hartmann, L., Chiang, H.-F., et al. 2013b, *ApJ*, 771, 48
- Zapata, L. A., Loinard, L., Rodríguez, L. F., et al. 2013, *ApJL*, 764, L14